Aalto University

OPEN ACCESS

This is an electronic reprint of the original article.
This reprint may differ from the original in pagination and typographic detail.

Schafer, Maximilian; Prawda, Karolina; Rabenstein, Rudolf; Schlecht, Sebastian J.

Distribution of Modal Damping in Absorptive Shoebox Rooms

Published in:
Proceedings of the 2023 IEEE Workshop on Applications of Signal Processing to Audio and Acoustics, WASPAA 2023

DOI:
10.1109/WASPAA58266.2023.10248145

Published: 01/01/2023

Document Version
Peer-reviewed accepted author manuscript, also known as Final accepted manuscript or Post-print

Please cite the original version:
Schafer, M., Prawda, K., Rabenstein, R., & Schlecht, S. J. (2023). Distribution of Modal Damping in Absorptive Shoebox Rooms. In *Proceedings of the 2023 IEEE Workshop on Applications of Signal Processing to Audio and Acoustics, WASPAA 2023* (IEEE Workshop on Applications of Signal Processing to Audio and Acoustics; Vol. 2023-October). IEEE. https://doi.org/10.1109/WASPAA58266.2023.10248145

This material is protected by copyright and other intellectual property rights, and duplication or sale of all or part of any of the repository collections is not permitted, except that material may be duplicated by you for your research use or educational purposes in electronic or print form. You must obtain permission for any other use. Electronic or print copies may not be offered, whether for sale or otherwise to anyone who is not an authorised user.

DISTRIBUTION OF MODAL DAMPING IN ABSORPTIVE SHOEBOX ROOMS

Maximilian Schäfer [1,*†] *Karolina Prawda*[2,*], *Rudolf Rabenstein*[1,*], *Sebastian J. Schlecht*[2,*‡]
[1]Friedrich-Alexander-Universität Erlangen-Nürnberg, Erlangen, Germany
[2]Acoustics Lab, Dpt. of Information and Communications Engineering, Aalto University, Finland

ABSTRACT

The image-source method is widely applied to compute room impulse responses (RIRs) of shoebox rooms with arbitrary damping. However, with increasing RIR lengths, the number of image sources grows rapidly, leading to slow computation. We propose a method to estimate the damping density of a damped shoebox room, which in turn can provide the energy decay necessary to model the stochastic late reverberation. The damping density is derived from a modal decomposition that is compliant with the ISM solution. We show that the proposed method gives a more accurate estimate of the energy decay than previous methods and can be efficiently computed regardless of the RIR lengths. While we focus on the derivation and evaluation, the main practical applications of the proposed model include, e.g., the faster synthesis of late reverb and the analysis of multi-slope decays.

Index Terms— Reverberation, Modal Decomposition, Image Source Method, Damping Density, Shoebox Rooms

1. INTRODUCTION

Accurate modeling of room impulse responses (RIRs) is important in numerous room acoustics and signal processing applications, such as source separation, dereverberation [1], and room acoustic simulations [2]. One of the most common approaches to simulate an RIR of a shoebox room is the image-source method (ISM) [3, 4].

After a certain time from the direct sound, called *transition time*, [5] and above a frequency threshold called *Schroeder frequency* [6, 5] RIRs can be described statistically, and stochastic reverberation models apply [1, 5, 7, 8]. Lehmann and Johansson proposed a particular solution to approximating the ISM solution of the damped shoebox room [9, 10, 11]. Such an approach is favorable for late reverberation, where ISM requires high computational costs to provide accurate results.

One of the frequent problems in room acoustic measurements is the presence of multi-slope decays, which may impair the estimation of certain acoustic parameters, such as reverberation time and sound-absorption coefficient [12, 13]. Therefore, determining the number of slopes in RIR's decay is often crucial. In the literature, the number of different decay times, and thus slopes, is defined based on the modal representation of RIRs. The modes are grouped according to either their type [14, 15] or incidence angle [16, 17], and each mode group is assigned its dominant decay time. Kuttruff suggested that the damping density might also be a good indicator of multi-slope decay [6]. The damping density is derived from the modal decomposition of the wave equation, describing the system's physics [18, 19]. Classic solutions for the modal decomposition of lossless and lossy shoebox rooms were given in [20, 21].

In this work, we derive the damping density distribution of a damped shoebox room. The derivation relies on a particular approximation of the modal decomposition compliant with the ISM solution. We further give fast approximations to the modal excitation term. The damping density gives direct access to the decay rates of a damped shoebox room.

As an application, we propose a fast method to obtain multi-slope decay characteristics of the late reverb that shows good agreement with ISM. A comparison with a previous method [9] shows an improved prediction of reverberation time.

The paper is organized as follows. Section 2 introduces the damping density and problem formulation. Section 3 presents the basics of modal and ISM solutions to the damped shoebox. Section 4 proposes a novel modal approximation and the resulting damping density, including fast approximations. Section 5 presents the evaluation results and a comparison to ISM and a fast ISM approximation.

2. PROBLEM DEFINITION

In this section, we define the damping density [20]. The RIR is a sum of individual modes, i.e.,

$$h(t) = \sum_n c_n \exp\left(\sigma'_n t\right) \cos\left(\omega'_n t - \phi_n\right), \quad \text{for } t \geqslant 0, \tag{1}$$

where t is time and $c_n, \sigma'_n, \omega'_n, \phi_n$, denote excitation factors, damping constants, frequency, and phase of individual modes, respectively. An expression proportional to the energy density is obtained by squaring $h(t)$

$$\begin{aligned} w(t) \propto [h(t)]^2 = &\sum_n \sum_m c_n c_m \exp\left[\left(\sigma'_n + \sigma'_m\right) t\right] \\ &\times \cos\left(\omega'_n t - \phi_n\right) \cos\left(\omega'_m t - \phi_m\right). \end{aligned} \tag{2}$$

By short-time averaging, the products with $n \neq m$ cancel such that

$$w(t) = \frac{1}{2} \sum_n c_n^2 \exp\left(2\sigma'_n t\right). \tag{3}$$

For a large number of modes, we can approximate the power response with a *damping density* $H(\sigma)$, i.e.,

$$w(t) = \int_{-\infty}^{0} H(\sigma) \exp(2\sigma t) \mathrm{d}\sigma. \tag{4}$$

Schroeder backward integration of the power response then yields the energy decay curve (EDC), i.e.,

$$\mathrm{EDC}(t) = \int_t^{\infty} w(\tau)\, \mathrm{d}\tau. \tag{5}$$

In the following, we propose a method to compute the damping density $H(\sigma)$ for a damped shoebox room compatible with the ISM solution. Fig. 1 shows the conceptual overview of the proposed method.

*Equal Contribution

†The work of M. Schäfer was supported by the Bavarian State Ministry of Science and Arts within the bidt Graduate Center for Postdocs.

‡Sebastian J. Schlecht is also at Media Lab, Dpt. of Art and Media, Aalto University, Finland.

979-8-3503-2372-6/23/$31.00 ©2023 IEEE

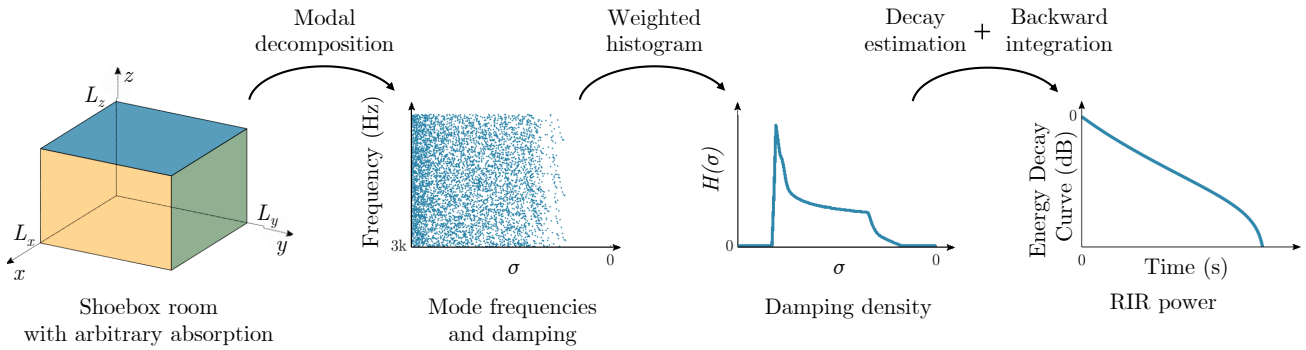

Figure 1: Conceptual overview of this paper. From left to right: a shoebox room with dimensions $L_\mathrm{x}, L_\mathrm{y}, L_\mathrm{z}$ and volume $V = L_\mathrm{x} L_\mathrm{y} L_\mathrm{z}$, having non-rigid walls, each characterized by a frequency-independent reflection factor r. We obtain mode frequencies and damping by using modal decomposition. From those, we acquire damping density $H(\sigma)$ by the means of weighted histogram. In the end, the RIR's EDC is estimated from $H(\sigma)$ by decay estimation (4) and backward integration (5).

3. ROOM ACOUSTICS

3.1. Modal Decomposition of Shoebox Room

A shoebox room in 3D space $\boldsymbol{x} = [x, y, z]$ is shown in Fig. 1, with spatial domain Ω, boundary $\partial\Omega$ and volume size $V = L_\mathrm{x} L_\mathrm{y} L_\mathrm{z}$

$$\Omega := \{\boldsymbol{x} | 0 \leqslant x \leqslant L_\mathrm{x}, 0 \leqslant y \leqslant L_\mathrm{y}, 0 \leqslant z \leqslant L_\mathrm{z}\}\,. \tag{6}$$

The time-dependent sound pressure $p(\boldsymbol{x}, t)$ is given by the three-dimensional wave equation as follows

$$\partial_{tt} p(\boldsymbol{x}, t) + c^2 \nabla^2 p(\boldsymbol{x}, t) = 0, \tag{7}$$

where ∂_{tt} denotes a second order time derivative, c is the speed of sound and ∇^2 is the Laplacian spatial differentiation operator. The solution to (7) requires a proper set of initial and boundary conditions for the sound pressure p and its derivatives [22, 18]. A general form of the solution for (7) is provided by the Green's function

$$p(\boldsymbol{x}, t) = \int_\Omega g(\boldsymbol{x}|\boldsymbol{\xi}, t) \overset{t}{*} f_\mathrm{ext}(\boldsymbol{\xi}, t) \mathrm{d}\boldsymbol{\xi}, \tag{8}$$

where $\overset{t}{*}$ denotes a convolution w.r.t. time, f_ext is a source term, and $g(\boldsymbol{x}|\boldsymbol{\xi}, t)$ is the Green's function

$$g(\boldsymbol{x}|\boldsymbol{\xi}, t) = \sum_{n=-\infty}^{\infty} \frac{\Lambda_n}{V} \mathrm{e}^{s_n t} \phi_n(\boldsymbol{x}) \phi_n(\boldsymbol{\xi}). \tag{9}$$

Hereby, functions ϕ_n are eigenfunctions of the spatial differentiation operator in (7) whose exact form is determined by the shape of Ω and the boundary conditions. The values s_n are the corresponding eigenvalues of ϕ_n defining the discrete spectrum of (7) and Λ_n are modal weighting factors [22, 19]. The eigenvalues $s_n = \sigma'_n \pm \mathrm{j}\omega'_n$ are counted by the discrete index $n \in \mathbb{Z}$; their real part is the damping constant σ'_n and their imaginary part the frequency ω'_n.

We assume an impulsive excitation at $\boldsymbol{x}_\mathrm{s}$ at $t = 0$, i.e., $f_\mathrm{ext}(\boldsymbol{x}, t) = \delta(\boldsymbol{x} - \boldsymbol{x}_\mathrm{s})\delta(t)$. Inserting f_ext into (8), exploiting the sifting property of the delta impulse [23], and considering the occurrence of the s_n-values in complex conjugated pairs, the sound pressure can be expressed as a multi-dimensional equivalent of (1)

$$p(\boldsymbol{x}, t) = \sum_{n=1}^{\infty} c_n(\boldsymbol{x}, \boldsymbol{x}_\mathrm{s}) \exp\left(\sigma'_n t\right) \cos\left(\omega'_n t\right), \tag{10}$$

with the excitation factors $c_n(\boldsymbol{x}, \boldsymbol{x}_\mathrm{s}) = 2\frac{\Lambda_n}{V} \phi_n(\boldsymbol{x}) \phi_n(\boldsymbol{x}_\mathrm{s})$. The DC-term with index $n = 0$ has been omitted. Finally, the damping density $H(\sigma)$ can be obtained from the Green's function g by inserting c_n and σ'_n from (10) into (3).

For a lossless shoebox room with rigid walls, i.e., the normal components of the particle velocity vanish at the surface of the walls [20], the eigenvalues s_n in (9) are well known [20, Eq. (3.15)]

$$s_n = \pm \mathrm{j} c \pi \sqrt{\left(\kappa_\mathrm{x}/L_\mathrm{x}\right)^2 + \left(\kappa_\mathrm{y}/L_\mathrm{y}\right)^2 + \left(\kappa_\mathrm{z}/L_\mathrm{z}\right)^2}, \tag{11}$$

where $n = [\kappa_\mathrm{x}, \kappa_\mathrm{y}, \kappa_\mathrm{z}]$ is an index tuple comprising counting variables for the three coordinate directions. Hence, different mode types are represented by different non-zero entries in n, i.e., axial modes in x, y, or z-direction have one, tangential two, and oblique modes three non-zero components, respectively. Similar to the eigenvalues, the eigenfunctions ϕ for the lossless case can be obtained straightforwardly from (7) and are well known

$$\phi_n(\boldsymbol{x}) = \cos(\kappa_\mathrm{x} \pi x / L_\mathrm{x}) \cos(\kappa_\mathrm{y} \pi y / L_\mathrm{y}) \cos(\kappa_\mathrm{z} \pi z / L_\mathrm{z}). \tag{12}$$

The modal weighting factors Λ_n are obtained from the orthogonality of the eigenfunctions ϕ_n and introduce different weighting dependent on the mode type, i.e., $\Lambda_n = 2, 4, 8$ for axial, tangential, and oblique modes, respectively.

3.2. Image Source Method

We compare the power response to the ISM [3] implemented in [4]. The RIR $h(t)$ is given by

$$\sum_{\substack{\mathbf{m}\in\mathcal{M} \\ \mathbf{p}\in\mathcal{P}}} r_{\mathrm{x}0}^{|m_x - q|} r_{\mathrm{x}1}^{|m_x|} r_{\mathrm{y}0}^{|m_y - j|} r_{\mathrm{y}1}^{|m_y|} r_{\mathrm{z}0}^{|m_z - k|} r_{\mathrm{z}1}^{|m_z|} \frac{g_\mathrm{ext}(t - \frac{d}{c})}{4\pi d}, \tag{13}$$

where $\mathcal{M} = \{(m_x, m_y, m_z) : -N \leqslant m_x, m_y, m_z \leqslant N\}$, $\mathcal{P} = \{(q, j, k) : 0 \leqslant q, j, k \leqslant 1\}$, d is the distance of the image source. The excitation term $g_\mathrm{ext}(t)$ is often chosen as a Dirac impulse, which leads to undesired behavior such as a strong amplification of the low frequencies [9]. To remedy the amplification, the ISM RIR is high-passed as a post-processing step. Here, we use instead an alternative excitation term that is compliant with the modal decomposition. Assuming a volume velocity source with Fourier transform $Q(\omega)$, the Fourier transform of the excitation term is

$$G_\mathrm{ext}(\omega) = j\omega\, G_0\, Q(\omega), \tag{14}$$

where G_0 comprises additional constants [6, Chap. 1]. As is apparent from (14), the volume velocity source effectively applies a highpass to the ISM output, equivalent to time-domain differentiation.

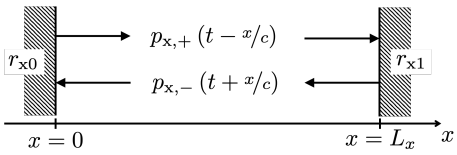

Figure 2: Travelling waves representation of the x-component of the sound pressure p with right $p_{\mathrm{x},+}$ and left travelling wave $p_{\mathrm{x},-}$, and the real-valued reflection factors $r_{\mathrm{x}0}$ and $r_{\mathrm{x}1}$ at $x = 0, L_{\mathrm{x}}$.

4. PROPOSED METHOD

The overview of the proposed method is given in Fig. 1 and Sec. 2 describes the individual steps of the procedure. In the following, we propose an approximation for the eigenvalues s_n of a damped shoebox room which is essential to obtain damping density $H(\sigma)$. Moreover, we propose a practical approximation that simplifies its computation.

For illustration, we present intermediate concepts with a running example room with dimensions $[L_{\mathrm{x}},\, L_{\mathrm{y}},\, L_{\mathrm{z}}] = [8.9, 6.3, 3.6]\mathrm{m}$, $c = 343\mathrm{m\,s^{-1}}$, and reflection factors $[r_{\mathrm{x}0},\, r_{\mathrm{x}1},\, r_{\mathrm{y}0},\, r_{\mathrm{y}1},\, r_{\mathrm{z}0},\, r_{\mathrm{z}1}] = [0.85, 0.97, 0.9, 0.97, 0.97, 0.75]$. The sampling frequency is 8 kHz.

4.1. Eigenvalue Approximation for a Lossy Shoebox Room

To compute the RIR and damping density for a lossy shoebox room, the excitation factors c_n and the eigenvalues $s_n = \sigma'_n \pm \mathrm{j}\omega'_n$ have to be derived from (7). In general, frequency-dependent wall impedances have to be considered. In this case, the eigenvalues s_n of (7) have to be obtained from a set of non-linear equations whose numerical solution is cumbersome and provides little insight [21]. However, under certain assumptions, e.g., real-valued wall impedances or large reflection factors, useful approximations for these general equations have been proposed, see, e.g., [20, Sec. 3.3]. In the following, we derive an approximation for eigenvalues s_n in (9) which is straightforward to obtain yet sufficiently accurate to approximate the RIR and damping density $H(\sigma)$ of a lossy shoebox room when compared to ISM.

As shown in Fig. 1, we assume that the damping in the shoebox room is characterized by frequency-independent reflection factors r, e.g., $r_{\mathrm{x}0}$ at $x = 0$ and $r_{\mathrm{x}1}$ at $x = L_{\mathrm{x}}$ at the walls in x-direction (see Fig. 2). Moreover, we assume that sound pressure p in (7) is separable to $p(\boldsymbol{x}, t) = p_{\mathrm{x}}(x,t)p_{\mathrm{y}}(y,t)p_{\mathrm{z}}(z,t)$, where p_{x}, p_{y} and p_{z} are the components of p in x, y and z-direction, respectively. This separation allows decomposing (7) into three equations, where the one in x-direction reads in the frequency domain

$$c^2 P_{\mathrm{x}}(x,s) - s_{\mathrm{x}}^2 P_{\mathrm{x}}(x,s) = 0, \tag{15}$$

with the Laplace-transform $P_{\mathrm{x}}(x,s) = \mathcal{L}\{p_{\mathrm{x}}(x,t)\}$. Similar equations exist for the y and z-direction. The values s_{x} as well as s_{y} and s_{z} for the other directions are related to s_n by

$$s_n = -|s_n| e^{-\mathrm{j}\varphi/2} = -\sqrt{s_{\mathrm{x}}^2 + s_{\mathrm{y}}^2 + s_{\mathrm{z}}^2} = \sigma'_n \pm \mathrm{j}\omega'_n. \tag{16}$$

We can solve (15) in terms of travelling waves, i.e.,

$$P_{\mathrm{x}}(x,s) = P_{\mathrm{x},+}(s)\mathrm{e}^{-s_{\mathrm{x}}\frac{x}{c}} + P_{\mathrm{x},-}(s)\mathrm{e}^{s_{\mathrm{x}}\frac{x}{c}}, \tag{17}$$

where $P_{\mathrm{x},+}$ and $P_{\mathrm{x},-}$ are the frequency domain equivalents of the right $p_{\mathrm{x},+}$ and left $p_{\mathrm{x},-}$ travelling waves, respectively (see Fig. 2). In order to obtain s_{x}, we have to define boundary conditions for (17). Therefore, we assume that the reflected wave at one wall is a weighted version of the incident wave

$$P_{\mathrm{x},+}(s) = r_{\mathrm{x}0} P_{\mathrm{x},-}(s), \qquad x = 0, \tag{18}$$

$$P_{\mathrm{x},-}(s)\mathrm{e}^{s_x \frac{L_x}{c}} = r_{\mathrm{x}1} P_{\mathrm{x},+}(s)\mathrm{e}^{-s_x \frac{L_x}{c}}, \qquad x = L_{\mathrm{x}}. \tag{19}$$

Inserting (18) into (19) and solving for s_{x} yields the x-contribution to the eigenvalues s_n in (16) as follows

$$s_{\mathrm{x}}(\kappa_{\mathrm{x}}) = \frac{\rho_{\mathrm{x}}}{2T_{\mathrm{x}}} + \mathrm{j}\frac{\pi\kappa_{\mathrm{x}}}{T_{\mathrm{x}}}, \tag{20}$$

where $\rho_{\mathrm{x}} = \ln(r_{\mathrm{x}0} r_{\mathrm{x}1})$ contains the reflection factors and $T_{\mathrm{x}} = L_{\mathrm{x}}/c$ is the travel time in x-direction. Similar calculations are done for the y and z components of P yielding the y and z-contributions of the eigenvalues s_n, i.e.,

$$s_{\mathrm{y}}(\kappa_{\mathrm{y}}) = \frac{\rho_{\mathrm{y}}}{2T_{\mathrm{y}}} + \mathrm{j}\frac{\pi\kappa_{\mathrm{y}}}{T_{\mathrm{y}}}, \qquad s_{\mathrm{z}}(\kappa_{\mathrm{z}}) = \frac{\rho_{\mathrm{z}}}{2T_z} + \mathrm{j}\frac{\pi\kappa_{\mathrm{z}}}{T_{\mathrm{z}}}, \tag{21}$$

with $\rho_{\mathrm{y}} = \ln(r_{\mathrm{y}0} r_{\mathrm{y}1})$ and $\rho_{\mathrm{z}} = \ln(r_{\mathrm{z}0} r_{\mathrm{z}1})$, and travel times $T_{\mathrm{y}} = L_{\mathrm{y}}/c$ and $T_{\mathrm{z}} = L_{\mathrm{z}}/c$. Finally, an approximation for the lossy eigenvalues s_n is obtained by inserting (20) and (21) into (16).

The proposed approximation of s_n is based on solving separate one-dimensional equations for the contributions s_{x}, s_{y}, and s_{z}, while their inherent coupling is not considered comprehensively. Therefore, the approximation is valid for axial modes, but it does not represent tangential and oblique modes in a physically correct way.

The RIR is obtained from the modes by (10). The eigenvalues $s_n = \sigma'_n \pm \omega'_n$ can be obtained by inserting (20) and (21) into (16). However, to obtain the excitation factors c_n, the eigenfunctions ϕ_n and the modal weighting factors Λ_n are necessary (see (10)). Assuming that the influence of the damping on the mode shapes and types is small for individual modes, we use the ϕ_n and Λ_n values from the lossless case as a sufficiently good approximation for the actual eigenfunctions and weighting factors [20, 21, 24]. Fig. 3 shows the close correspondence of the RIR obtained by the ISM (13) and the modal synthesis (10) with the proposed eigenvalue approximation from (20) and (21).

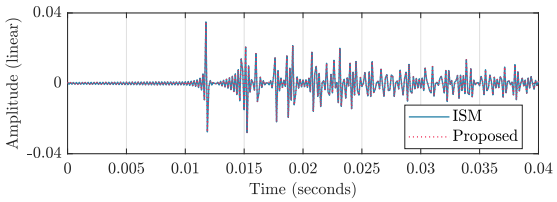

Figure 3: Comparison of RIR computed with the ISM and the proposed modal decomposition for the example shoebox room.

4.2. Damping Density

The damping density $H(\sigma)$ is computed from damping constants σ and the excitation factors c_n of the modal decomposition as a weighted histogram, i.e.,

$$H(\sigma)\mathrm{d}\sigma = \sum_{\sigma < \sigma'_n < \sigma + \mathrm{d}\sigma} c_n^2, \tag{22}$$

where $\mathrm{d}\sigma$ is the bin width. In the following, we show that the computation of $H(\sigma)$ in (22) can be further simplified.

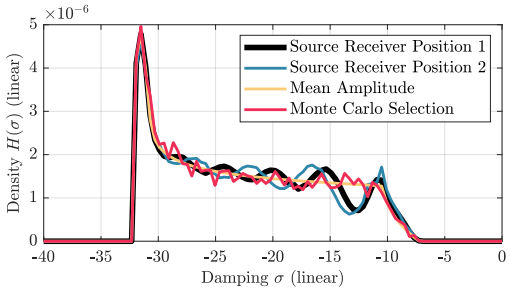

Figure 4: Comparison of different approximations of $H(\sigma)$ for the example shoebox room with three damped walls: Full histogram with (4) for two different receiver positions (black, blue); with mean excitation factors (24) (yellow); with Monte Carlo sampling (red).

The excitation factors c_n depend on the mode type. For high sampling frequency, the oblique modes dominate the superposition of modes (3). In the example room, for a sampling frequency of 8 kHz, the axial modes are less than 0.01 %, and tangential modes are less than 2 % of the total number of modes. Thus, we assume for the approximation that all modes are oblique, i.e., $\overline{\Lambda}_n = 8$. Moreover, the excitation factors c_n strongly depend on the source and receiver position (see also (10)). Instead, we can use a spatial mean of the positional factor, i.e.,

$$\langle \phi_n^2(\boldsymbol{x}) \rangle = 1/8, \tag{23}$$

for $\kappa_\mathrm{x}, \kappa_\mathrm{y}, \kappa_\mathrm{z} > 0$, yielding the following mean excitation factor

$$\langle c_n(\boldsymbol{x}) \rangle = 2\frac{\overline{\Lambda}_n}{V} \langle \phi_n(\boldsymbol{x}) \rangle \langle \phi_n(\boldsymbol{x}_\mathrm{s}) \rangle = \frac{1}{4V}. \tag{24}$$

Thus, (22) becomes a simple counting histogram. Fig. 4 shows damping density $H(\sigma)$ derived from the actual excitation factors c_n of two different source-receiver-positions and with the mean weighting factors in (24). It can be observed that the mean excitation factor provides a sufficient approximation.

For increasing frequency, also the number of modes needed to estimate $H(\sigma)$ becomes excessive. In the example room, there are more than 10 million modes below 8 kHz. To further accelerate the computation of (22), we employ a Monte Carlo sampling. The results are also shown in Fig. 4. We observe, that the damping density $H(\sigma)$ estimated from 0.1 % of randomly selected modes results in a close approximation for the actual damping density.

5. APPLICATIONS AND EVALUATION

The damping density $H(\sigma)$ is a useful mid-level representation for various room acoustic tasks. For instance, the damping density can be employed to infer the (possibly multi-slope) decay behavior of the reverberation tail [13]. This is confirmed by Fig.4, which shows that the decay is not a single slope, but inherently has a wide distribution of different decays.

Next, we consider a fast synthesis of the stochastic late reverberation application similar to Lehmann and Johansson [9]. Following the steps in Fig.1, damping density $H(\sigma)$ is estimated by computing the histogram of σ_n for randomly selected indices n, see (22) and (24). By applying (4), the power response $w(t)$ is computed. The late reverberation is synthesized as $w(t)v(t)$, where $v(t)$ is Gaussian white noise. The most costly step to estimate $H(\sigma)$ is the computation of s_n-values (16) for sufficiently many n. For this example, we used 100k samples. In comparison, ISM needs to sum around 10 million pulses with fractional delays for 2 seconds of response. Our implementation in Matlab is 10 times faster than ISM [4] [1].

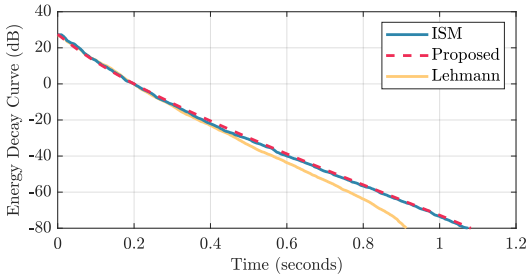

Figure 5: Comparison of EDCs for ISM (blue), Lehmann (yellow), and the proposed method (red) for the example shoebox room with three damped walls (see Sec. 4).

Table 1: $T_{X,\mathrm{diff}}$ values for Lehmann and proposed approximation compared to ISM (percentage of target values).

Measure	Method	Mean	Std. dev.	Max	Min
$T_{30,\mathrm{diff}}$	Proposed [%]	2.9	2.6	11.9	0.1
	Lehmann [%]	6.2	5.4	22.6	0.2
$T_{60,\mathrm{diff}}$	Proposed [%]	3.8	3.3	16.0	0.1
	Lehmann [%]	8.9	7.1	27.9	0.1

Figure 5 compares the EDCs between the ISM, Lehmann [9] approximation, and the proposed method. We observe that the EDC estimated with the proposed method is in excellent agreement with the results from ISM. This confirms that the proposed method improves upon Lehmann's method.

In the following, we confirm and generalize our results by a random sampling of parameters. The proposed method was tested against the ISM and Lehmann's method on 100 shoebox rooms with dimensions L randomly chosen between 3 and 13 m, reflection factors r randomly chosen from 0.7–0.97 range, and random source and receiver positions (at least 0.5 m from the nearest surface). We compared Lehmann's and the proposed method in terms of T_{30} and T_{60} decay times, where ISM served as the ground truth.

The results are shown in Table 1 for the proposed method and Lehmann's method, as a difference between T_{30} and T_{60} values obtained with tested methods and ISM, according to $T_{X,\mathrm{diff}} = 100 \times |T_{X,\mathrm{approx.}} - T_{X,\mathrm{ISM}}|/T_{X,\mathrm{ISM}}$, where $X = 30, 60$. The results show that in a number of diverse scenarios, the proposed method is performing better than the Lemann method, being closer to the results of ISM. Moreover, the proposed method exhibits a more stable behavior, without extreme deviations from ISM.

6. CONCLUSION

This paper proposes a novel derivation of the damping density of damped shoebox rooms from room mode statistics. An approximation of the modal decomposition is derived, which complies with the ISM solution. The damping density can be estimated efficiently using oblique modes, the mean positional excitation, and Monte Carlo sampling. We show that the resulting energy decay has a close match and improves upon a previous approximation.

In future work, the damping density can be used to study multi-slope decay directly by avoiding the inverse problem of fitting to the energy decay curve. Further, a directional extension of the damping density can possibly be developed.

[1] The source code of our implementation can be found on [25]

7. REFERENCES

[1] A. Aknin and R. Badeau, "Stochastic reverberation model with a frequency dependent attenuation," in *IEEE Workshop on Applications of Signal Processing to Audio and Acoustics (WASPAA)*, New Paltz, NY, USA, 2021.

[2] L. Savioja and U. P. Svensson, "Overview of geometrical room acoustic modeling techniques," *J. Acoust. Soc. Am.*, vol. 138, no. 2, pp. 708 – 730, 08 2015.

[3] J. B. Allen and D. A. Berkley, "Image method for efficiently simulating small-room acoustics," *J. Acoust. Soc. Am.*, vol. 65, no. 4, pp. 943 – 950, 1979.

[4] E. A. P. Habets, "Room Impulse Response Generator," Technische Universiteit Eindhoven, Tech. Rep., 2006.

[5] R. Badeau, "Common mathematical framework for stochastic reverberation models," *The Journal of the Acoustical Society of America*, vol. 145, no. 4, pp. 2733–2745, 2019.

[6] H. Kuttruff, *Room Acoustics, Fifth Edition*, ser. CRC Press. CRC Press, 06 2009.

[7] R. Badeau, "Unified Stochastic Reverberation Modeling," ser. European Signal Processing Conference (EUSIPCO), 09 2018, pp. 1 – 5. [Online]. Available: https://hal.archives-ouvertes.fr/hal-01795319/document

[8] A. Aknin, T. Dupré, and R. Badeau, "Evaluation Of A Stochastic Reverberation Model Based On The Image Source Principle," in *Proceedings of the 23rd International Conference on Digital Audio Effects (DAFx2020)*, Vienna, Austria, 2020.

[9] E. A. Lehmann and A. M. Johansson, "Diffuse Reverberation Model for Efficient Image-Source Simulation of Room Impulse Responses," *IEEE/ACM Trans. Audio, Speech, Language Process.*, vol. 18, no. 6, pp. 1429 – 1439, 2010-08. [Online]. Available: http://ieeexplore.ieee.org/document/5299028/

[10] E. A. Lehmann, A. M. Johansson, and S. Nordholm, "Reverberation-Time Prediction Method for Room Impulse Responses Simulated with the Image-Source Model," ser. Proc. IEEE Workshop Applicat. Signal Process. Audio Acoust. (WASPAA), 2007, pp. 159 – 162. [Online]. Available: http://ieeexplore.ieee.org/document/4392980/

[11] E. A. Lehmann and A. M. Johansson, "Prediction of energy decay in room impulse responses simulated with an image-source model," *J. Acoust. Soc. Am.*, vol. 124, no. 1, pp. 269 – 277, 2008-07. [Online]. Available: http://asa.scitation.org/doi/abs/10.1121/1.2936367?journalCode=jas

[12] F. V. Hunt, "The absorption coefficient problem," *J. Acoust. Soc. Am.*, vol. 11, no. 1, pp. 38–40, 1939.

[13] J. Balint, F. Muralter, M. Nolan, and C.-H. Jeong, "Bayesian decay time estimation in a reverberation chamber for absorption measurements," *The Journal of the Acoustical Society of America*, vol. 146, no. 3, pp. 1641–1649, 2019.

[14] F. Jacobsen and P. M. Juhl, *Fundamentals of general linear acoustics*. John Wiley & Sons, 2013.

[15] M. Meissner, "Prediction of reverberant properties of enclosures via a method employing a modal representation of the room impulse response," *Arch. Acoust.*, vol. vol. 41, no. No 1, pp. 27–41, 2016.

[16] F. V. Hunt, L. L. Beranek, and D. Y. Maa, "Analysis of Sound Decay in Rectangular Rooms," *J. Acoust. Soc. Am.*, vol. 11, no. 1, pp. 80–94, 1939.

[17] M. Berzborn, J. Balint, and M. Vorländer, "On the estimation of directional decay times in reverberation rooms," in *Proc. Euronoise 2021*, 2021.

[18] R. Rabenstein and M. Schäfer, *Multidimensional Signals and Systems - Theory and Foundations*. Springer Cham, 2023.

[19] R. F. Curtain and H. J. Zwart, *An Introduction to Infinite-Dimensional Systems Theory*. New York: Springer-Verlag, 1995.

[20] H. Kuttruff, "Eigenschaften und Auswertung von Nachhallkurven," *Acta Acustica united with Acustica*, vol. 8, no. 4, pp. 273 – 280, 1958. [Online]. Available: http://www.ingentaconnect.com/content/dav/aaua/1958/00000008/A00104s1/art00006?crawler=true

[21] P. Filippi, D. Habault, J. Lefebvre, and A. Bergassoli, *Acoustics: Basic Physics, Theory and Methods*. Academic Press, 1999.

[22] R. V. Churchill, *Operational Mathematics*. Boston, Massachusetts: Mc Graw Hill, 1972.

[23] A. Oppenheim and R. Schäfer, *Discrete-Time Signal Processing*, 3rd ed. Pearson, 2021, e-book.

[24] P. Svensson, J. Botts, and L. Savioja, "Computational modeling of room acoustics i: Wave-based modeling," in *Architectural Acoustics Handbook*, N. Xiang, Ed. Plantation, FL: J. Ross Publishing, 2017, ch. 1.

[25] M. Schäfer, K. Prawda, R. Rabenstein, and S. J. Schlecht, "Source Code: Distribution of Modal Damping in Absorptive Shoebox Rooms," https://github.com/SebastianJiroSchlecht/ShoeboxModalDampingDistribution, 2023.